Research Square

Preprints are preliminary reports that have not undergone peer review.
They should not be considered conclusive, used to inform clinical practice,
or referenced by the media as validated information.

BCG enables protection against malaria through adjuvanting an Adenovirus-vectored vaccine

Sören Reinke
The Jenner Institute, University of Oxford
Marta Ulaszewska
The Jenner Institute, University of Oxford
Qi Su
University of Oxford
Lee Sims
The Jenner Institute, University of Oxford
Romain Guyon
The Jenner Institute, University of Oxford
Adam Truby
The Jenner Institute, University of Oxford
Jelena S. Bezbradica
University of Oxford
Joannah R. Fergusson
University of Oxford
Anita Milicic
anita.milicic@ndm.ox.ac.uk

The Jenner Institute, University of Oxford

Short Report

Keywords: Vaccine, Viral Vector, AdHu5, BCG, Malaria

Posted Date: October 22nd, 2025

DOI: https://doi.org/10.21203/rs.3.rs-7858925/v1

License: This work is licensed under a Creative Commons Attribution 4.0 International License.
Read Full License

Additional Declarations: No competing interests reported.

Version of Record: A version of this preprint was published at npj Vaccines on June 24th, 2026. See the published version at https://doi.org/10.1038/s41541-026-01506-9.

Abstract

The BCG vaccine against TB offers broader non-specific health benefits, including reduced malaria infection. This may stem from its ability to epigenetically imprint innate immune cells, enhancing subsequent response to pro-inflammatory stimuli, coupled with intrinsic adjuvanticity through direct activation of cell surface PRRs. Here we investigate whether vaccinating with BCG in parallel with an adenoviral-vectored vaccine could be beneficial for protection against malaria in a mouse model. We show that combining the two vaccines broadens and strengthens the early innate cytokine repertoire, enabling strong $CD8^+$ T cell-dependent protection. Our findings reveal co-immunisation with BCG and a viral vector as a promising strategy to combat both TB and malaria in double-endemic regions.

Main text

The tuberculosis (TB) vaccine Bacillus Calmette-Guérin (BCG) has well-documented off-target benefits against a broad range of infections, including malaria, sepsis, leprosy, SARS-CoV-2, and even as therapy in bladder cancer[1]. These non-specific effects are believed to be underpinned by epigenetic imprinting of myeloid cells[2], resulting in enhanced secretion of pro-inflammatory cytokines such as TNF and IL-1β for up to a few months post BCG vaccination[3].

BCG-induced non-specific immunity against malaria[4-8] is of particular significance as the endemic geographic regions of TB and malaria largely overlap[9]. Field studies in sub-Saharan Africa have shown association between BCG vaccination and reduced malaria prevalence in children under 5, and seasonal reductions in all-cause neonatal mortality[9,10]. To date, the protective effect of BCG has not been investigated in the context of malaria vaccination. In view of its specific adjuvant-like properties through pathogen recognition receptor (PRR) activation, along with the off-target effect on malaria, it is relevant to consider vaccination strategies that administer malaria and BCG vaccines at the same time or in temporal proximity, to exploit the full potential of BCG in reducing both malaria and TB burden in double-endemic regions.

This study explores the effect of BCG on the immune response elicited by an adenoviral-vectored malaria vaccine (human Adenovirus serotype 5, hereafter referred to as Ad), in a mouse model of malaria. The Ad construct encodes an immunodominant $CD8^+$ T cell epitope Pb9 from *Plasmodium berghei* (*P. berghei*) circumsporozoite protein, which mediates protection against liver-stage malaria in this mouse model[11-13].

Mice were immunised with a low dose of Ad (offering no protection), BCG alone, or with Ad+BCG (injected at different sites), and challenged with *P. berghei* malaria parasites 2-4 weeks later (Fig. 1a). Mice vaccinated with Ad or BCG alone had no protection against malaria (Fig. 1b), whereas 80% of the mice that received both vaccines developed strong sterile immunity (Fig. 1b). This suggests that BCG is adjuvanting the adaptive, Pb9 $CD8^+$ T cell driven, response against malaria either through innate immune imprinting or by directly adjuvanting the innate response to the Ad-vectored vaccine. To assess the role

of myeloid cell imprinting[14] in protection, mice were vaccinated with BCG two or four weeks prior to Ad vaccination. These regimens resulted in a lower survival rate compared to Ad-BCG co-administration (Fig S1a), suggesting that the key element in protection against malaria in this model is the direct BCG-adjuvanting effect of the Ad vaccine.

To mechanistically dissect the protective immune response and assess potential synergy between BCG and Ad in the context of liver-stage malaria, we phenotyped splenic and hepatic $CD8^+$ T cells[15] and analysed antibody (Ab) responses after vaccination with Ad, BCG and Ad+BCG (Fig.1a). Of note, a reduced percentage of $Pb9^+$ specific $CD8^+$ T cells was observed in the spleens and livers of mice receiving Ad+BCG compared to Ad alone (Fig 1c-e, S1b, c), replicating our previous findings with adjuvanted Ad vaccine in malaria protection[12]. Vaccination with BCG also affected the distribution of $Pb9^+$ $CD8^+$ T cell memory sub-populations, resulting in a higher proportion of central memory T cells (Tcm) and reduction in effector memory T cells (Tem) that with Ad vaccine alone (Fig. 1d). Importantly, immunisation with BCG did not affect the $CD8^+$ T cell surface density of the liver-homing cell marker CXCR6[16] (Fig S1b, c), which has previously been associated with protection against liver stage malaria in mice, and which we found to be more abundant on Pb9-specific T cells compared to the $Pb9^-CD8^+$ T cell subset (Fig S1b, c).

Given that the adaptive immunity against malaria generated by this vaccine is reliant solely on the Pb9 T cell epitope, the observed reduction in total antigen (Ag)-specific $CD8^+$ T cells suggests that BCG-induced perturbation of T cell memory subsets may be of significance, with the protection driven by the type (rather than the total number) of Ag-specific $CD8^+$ T cells. Antigen-specific Tcm, which were enriched after Ad+BCG vaccination, have also previously been demonstrated to enhance sterile protection in this model[12]. Indeed, the efficiency of the $CD8^+$ T cell response relies on the quantity/density of the presented Ag, as well as the quality of co-stimulation by the myeloid antigen presenting cells which are targets of BCG activation[17].

Investigating the effect of Ad and BCG co-administration on generating B cells and Ab responses, we found a reduction in the total number of germinal centre B cells and plasma cells in mice that received Ad+BCG, compared to Ad alone (Fig. 1f-h). Likewise, immunisation with Ad+BCG led to a slight reduction in the overall numbers of plasmablasts and memory B cells, compared to Ad alone (Fig. S2a-c). To investigate if addition of BCG might have resulted in a weakened Ab response against the Ad vaccine, which encodes GFP as a surrogate Ag, we measured anti-GFP IgG titres post vaccination. Akin to our T cell data, additional immunisation with BCG did not affect Ag-specific IgG titres, indicating that despite a reduction in the number of circulating lymphocytes, BCG has the capacity to generate more effective B cells (Fig. 1i). In parallel, the addition of the Ad vaccine enhanced the anti-BCG humoral response, and increased seroconversion against BCG in the Ad+BCG group compared to BCG alone. (Fig. 1g, 1j). These findings suggest a reciprocal adjuvanting effect between Ad and BCG, indicating that simultaneous vaccination with BCG and viral-vectored vaccines could enhance protection against both TB and the disease targeted by the vectored vaccine.

Activation of innate immunity by BCG is well documented[17], and could play a key mechanistic role in the observed effect of BCG on the adaptive response to the Ad-vectored vaccine. We profiled the early innate responses to the three vaccination regimens (Ad, BGC, Ad+BCG), by analysing the cytokine secretion patterns at the site of injection (SOI), and systemically, in the serum and the spleen (Fig. 2a). There was a clear difference in systemically induced cytokines between Ad and BCG, with Ad inducing IFN-γ, IFN-α and CXCL-10 secretion, and BCG promoting production of CXCL1 and IL-6 (Fig. 2b, c, S3). This effect was particularly pronounced in the serum. Simultaneous vaccination with Ad and BCG resulted in a broader, merged, pattern of secreted cytokines (Fig 2b, S3), supporting the premise of BCG-promoted adjuvantation through expanding the pro-inflammatory cytokine spectrum. Locally, in the muscle (SOI), additional cytokines were induced by Ad (CCL5) or BCG (CCL2, IL-1β, GM-CSF, TNF, Fig. 2d, S3) which were not detected systemically. Interestingly, in Ad+BCG vaccinated mice, with Ad and BCG given into the opposite limbs, the vaccinated sites showed lower cytokine secretion compared to the respective single-vaccinated mice (Fig. 2d). However, this did not affect the cytokines on the systemic level, either qualitatively or quantitatively, as seen in the serum and the spleen (Fig. 2b, c, S3). Overall, our innate cytokine data are in line with previous findings from immunising with Ad[18] or BCG[19] alone, and reveal the induction of a pool of pro-inflammatory cytokines (IFN-γ, IFN-α, IL-6, IL-1β, TNF), chemo-attractants (CXCL1, CCL2, CCL5, CXCL10), and the colony-stimulating factor GM-CSF, when both vaccines are given at the same time.

To corroborate these findings in a human system, we utilised human macrophages derived from peripheral-blood $CD14^+$ monocytes by M-CSF stimulation. Activation of the NLRP3 inflammasome after in vitro stimulation with Ad, BCG or Ad+BCG (Fig 2e) was measured as a key indicator of adjuvanticity[20] and BCG-mediated imprinting[21]. Direct TLR stimulation of myeloid cells induces NFkB signalling, promoting TNF secretion and the expression and post-translational modifications of the NLRP3 inflammasome[20]. TLR priming also strongly induces the expression of pro-IL-1β, ready for inflammasome-mediated processing into the active form. Full inflammasome activation requires a second signal, typically delivered from pathogen or vaccine uptake, leading to the secretion of IL-1β and IL-18, and pro-inflammatory cell death[20]. Interestingly, in vitro, Ad and BCG individually induced low amounts of secreted IL-1β, and when combined led to a strong IL-1β secretion across a range of doses (Fig 2f). AdHu5 vector is known as a poor inducer of secreted IL-1β[22], indicating either lack of induction of pro-IL-1β, or absence of inflammasome activation. BCG can induce transcriptional upregulation of pro-IL-1β but only limited secretion of the active cytokine, in line with its recognised role as a modest activator of the inflammasome pathway[23]. Our data support this, demonstrating secreted IL-1β in the BCG- but not the Ad-vaccinated muscle (Fig 2c, S3).

Similarly, combined Ad+BCG stimulation strongly activated TNF secretion, which is induced by TLR signalling and independent of the inflammasome activation (Fig 2f). Inflammasome-dependent cell death, measured by the release of cytosolic enzyme lactate dehydrogenase (LDH), was found to be vaccine dose-dependent and only elevated at the highest concentrations of Ad+BCG (Fig 2f). These findings demonstrate that, in human macrophages, Ad and BCG strongly synergise in TLR and

inflammasome pathway activation which neither of the vaccines can achieve individually. As TLR and inflammasome activation are hallmarks of potent adjuvanticity[20] - a key contributor to effective vaccination - engagement of these pathways is likely to be beneficial for both vaccines.

In summary, we demonstrate that combining BCG with a viral-vectored malaria vaccine generates a broader innate immune response and enables protection against malaria challenge. Simultaneous administration of both vaccines induces a potent inflammatory cytokine profile, capable of supporting protective $CD8^+$ T cells in this challenge model. Recent studies in mice have shown that intravenously administered BCG can protect against SARS-CoV-2 via $CD4^+$ T cell mediated IFN-γ secretion, through imprinting of myeloid and epithelial cells for enhanced antiviral immunity[24,25]. In clinical trials, previous administration of BCG has been found to enhance the immune response to RNA- or viral vector-based SARS-CoV-2 vaccines[26,27]. Consequently, our findings broaden the portfolio of advantageous applications of the BCG vaccine, identifying co-administration of BCG and malaria vaccines as a potentially promising strategy to combat both TB and malaria in double-endemic regions.

Methods

Mice and Immunisations

For all experiments, mice were purchased from Envigo, UK. Animals were maintained at the Centre for Human Genetics, University of Oxford, housed under Specific Pathogen Free (SPF) conditions in individually ventilated cages, with constant temperature and humidity and a 12 hour light/dark cycle, and in accordance with the recommendations of the UK Animals (Scientific Procedures) Act 1986 and ARRIVE guidelines. Protocols were approved by the University of Oxford Animal Care and Ethical Review Committee for use under Project Licenses P9804B4F1 and PP0984913, granted by the UK Home Office.

Anaesthetised (using vaporized IsoFlo®) female BALB/c mice (BALB/cOlaHsd) mice, aged 7–10-weeks, were immunised intramuscularly (i.m.) with a total volume of 50 µL in the tibialis muscle. In the initial experiments BCG was administered intradermally (i.d.) into the ear (2 x 25 µL each site). Comparison with i.m. administration showed no difference in protection against malaria and BCG was given i.m. in subsequent experiments. Each vaccine dose contained 0.5×10^5 CFU BCG, or 5×10^7 i.u. AdHu5-TIPeGFP.

Sporozoite production

Plasmodium berghei (ANKA strain clone 234) sporozoites were produced as previously described[28]. Starved female *Anopheles stephensi* mosquitoes were fed for approximately 10 min on BALB/c mice infected with *P. berghei* parasites. The mosquitoes were then maintained on Fructose/PABA solution at 19–21°C in a humidified incubator on 12 h light/dark cycle. Approximately 21 days after feeding, the mosquitoes were dissected and the salivary glands removed. While keeping on ice, the glands were

placed in RPMI-1640 and disrupted with a tissue homogeniser to release the sporozoites. The sporozoites were counted using a haemocytometer, while keeping on ice to preserve viability, and immediately proceeded to malaria challenge.

Malaria challenge

Malaria challenge was performed as described previously[28]. For all experiments 1,000 *P. berghei* sporozoites (described above) were injected intravenously in a total volume of 100 µL into the lateral tail vein of each mouse. From day 5 post challenge the mice were monitored for infection by thin-film blood smear (fixed in methanol and stained in 10% Giemsa for 30 min). Mice were sacrificed when >1% parasitaemia was observed. If no parasites were detected on day 12 after challenge, mice were considered sterilely protected.

Ex-vivo IFN-γ splenocyte ELISpot

ELISpot assays were performed using the IFN-γ ELISpot (kit 3321-2A, Mabtech, UK) as described previously[28]. In brief, two weeks after immunisation mice were culled and spleens removed. Single cell suspensions were prepared by homogenising and straining the spleens followed by brief incubation in ACK lysis buffer to remove erythrocytes. Cells were washed with PBS, pelleted, resuspended in complete α-MEM and counted using the CASY cell counter. MultiScreen-IP 0.45 µm sterile plates were coated with 5 µg/ml rat anti-mouse interferon gamma mAb AN18 diluted in carbonate-bicarbonate buffer overnight at 4 °C. Plates were then blocked for at least one hour at 37 °C with complete α-MEM. Cells were plated and stimulated for 18–20 h with 1 µg/mL of Pb9 peptide. Plates were washed and incubated with 1 µg/mL biotinylated anti-mouse-IFNγ mAb R46A2, followed by incubation with 1 µg/mL streptavidin alkaline phosphatase. Spots were developed by addition of 50 µL per well of colour development buffer and counted using ELISpot software (AID). Results are expressed as spot forming cells (SFC) per million splenocytes after subtracting background responses in unstimulated wells.

Flow Cytometry

Phenotypic analysis of $CD8^+$ T cells was performed by surface marker staining using the following fluorescently labelled antibodies: PE-Cy7-CD11a (BD Bioscience cat #558191), PE-CD186 (Biolegend cat #151104), BV711-CD69 (Biolegend cat #104537), BV650-CD44 (Biolegend cat #103049), BV605-CD62L (Biolegend cat #104437), BV421-KLRG1 (Biolegend cat #138413), AF700-CD8 (Biolegend cat #100729). Non-specific Ab binding was prevented by incubation with anti-CD16/CD32 Fcγ III/II Receptor (BD Pharmingen, UK) prior to the surface staining. The Pb9 tetramer was provided by the NIH tetramer facility (MHC tetramer core facility, Emory University Vaccine Center, Atlanta, USA) using SYIPSAEKI peptide. Live and dead cells were distinguished using LIVE/DEAD^{TM} Fixable Aqua Dead Stain Kit (ThermoFisher Scientific, UK). To define subpopulation distribution within the $Pb9^+$ compartment (Figure

1d, e) cells were gated on singlets, size, $CD8^+$, $Pb9^+$, and subsequent definition of subpopulations as depicted in Figure S1d without gating on $CD44^+/CD11a^+$ as $Pb9^+$ cells were generally positive for these markers. Flow cytometric analyses were performed on LSRII (BD Biosciences, UK) and data analysed with FlowJo software.

For B cell profiling, freshly harvested splenocytes were seeded in 96-well plates at a density of ~$1.5x10^6$ cells per well in chilled FACS buffer. Cells were washed and stained with diluted nIR Zombie L/D stain (Biolegend cat #423105) and incubated for 15 minutes at room temperature. After incubation, cells were washed and stained with a cocktail of the following antibodies diluted in FACS buffer: BV421-CD19 (Biolegend cat #115549), BV605-B220 (Biolegend cat #130244), BV786-CD95 (BD Bioscience cat #740716), PerCPCy5.5-GL7 (Biolegend cat #144609), PECy5-CD38 (Invitrogen cat #15-0381-82), PECy7-CD138 (Biolegend cat #142513), AF700-IgD (Biolegend cat #405729), APCCy7-CD3 (Biolegend cat #100222), APCCy7-F4/80 (Biolegend cat #123117). Cells were subsequently washed and transferred to FACS tubes for flow cytometric analyses on a Fortessa (BD Biosciences, UK).

Total IgG ELISA

ELISAs to detect antibodies against eGFP (expressed by AdHu5-TIPeGFP) or total BCG were performed as previously described[28]. Serum was obtained by collecting blood from the lateral tail vein in a microcuvette tube. Blood was allowed to clot at 4 °C overnight before centrifugation at 13,000 rpm for 4 min and sera removed and stored at −20 °C until use. For total IgG ELISAs, Nunc-Immuno Maxisorp 96 well plates were coated with 1 µg/mL eGFP in carbonate-bicarbonate coating buffer or 10^5 CFU BCG per well overnight at 4 °C. Plates were washed with PBS-Tween (0.05% v/v) and blocked with 2% BSA in PBS-Tween for 1 h at RT. Sera were diluted appropriately between 1:200 and 1:3,200 (depending on Ag and time point) in 1% BSA in PBS-Tween and added to plate in duplicates. Plates were incubated for 2 h at room temperature and then washed as before. Fc-specific goat anti-mouse IgG conjugated to alkaline phosphatase (AP) (1 in 5,000, Sigma-Aldrich, A1418) was added for 1 h at room temperature (eGFP) or overnight at 4°C (BCG). Following a final wash, plates were developed by adding *p*-nitrophenylphosphate at 1 mg/mL in diethanolamine buffer and OD was read at 405 nm. Total IgG concentrations against eGFP or BCG in sera were calculated by interpolation against a standard curve generated from a serum pool of previously AdHu5-TIPeGFP or BCG immunised mice. Sera from naive mice were used as negative control.

ELISA for detection of cytokines in serum, spleen, and muscle (SOI)

Tissue cytokines were assessed as described previously[29]. To detect innate cytokines in serum, spleen and muscle (SOI) samples, mice were immunised with AdHu5-TIPeGFP and/or BCG as described above. At specific time points mice were sacrificed, and tissues harvested. Blood samples were allowed to clot for 2 h before centrifugation at 13,000 rpm for 4 min; sera were stored at −80 °C until use. Muscle and spleen samples were weighed, transferred into PBS supplemented with protease inhibitor (Roche,

11873580001), and dissociated in gentleMACS M Tubes using the gentleMACS Octo Dissociator. Cell suspensions were stored at −80°C. Before use, samples were thawed, clarified by centrifugation at 10,000 rpm for 5 min, and supernatants analysed for cytokines and chemokines using the mouse MU Anti-Virus Response Panel flow assay kit (LEGENDplex, Biolegend) according to the manufacturer's instructions. LSR Fortessa (BD) flow cytometer was used to assess fluorescence intensity of beads and data analysed using LEGENDplex Data Analysis Software Suite.

Human Monocyte Derived Macrophages (HMDM)

Assays on Human Monocyte Derived Macrophages were performed as previously described[29]. In brief, peripheral blood mononuclear cells were isolated using Ficoll gradient from healthy donors from NHS Oxford blood bank (REC approval 11/H0711/7). Magnetic beads (eBioscience, 8802-6834-74) were used to positively select $CD14^+$ monocytes which were differentiated into macrophages by culturing for 7 days with M-CSF (100 ng/mL, BioLegend, 574808). Cells were cultured in RPMI (Fisher, 21870076) with 10% FBS (Life Technologies, 16000044) and 1x Pen/Strep/Glutamine (Fisher, 10378016) at 37 °C with 5% CO_2, and supplemented with fresh media containing 100 ng/mL M-CSF on day 2 and day 5. After day 7 of differentiation, cells were re-plated (70,000 cells per well in flat bottom 96-well plates in 100 µL complete RPMI) and on day 8 cells were stimulated for inflammasome-activation experiments.

Differentiated HMDMs were plated at a density of $0.7x10^6$ cells/mL complete RPMI and stimulated for 24 h with AdHu5-TIPeGFP and/or BCG at concentrations indicated in the Figures. Culture media was replaced with 100 µL OptiMEM (Fisher, 31985062) immediately before stimulation. After cell stimulation, cell supernatants were collected for analysis. Secretion of IL-1β and TNF was measured in cell-free supernatants using ELISA (Thermo Fisher, 88-7261-77 and 88-7346-88) according to manufacturer's instructions. Cellular viability was assessed using cell culture supernatants and the Cytox96 nonradioactive cytotoxicity assay (Promega, G1780).

Statistical analysis

Statistical analysis was performed using Prism software (V10). Statistical tests applied and pairwise comparisons with correction for multiple testing are indicated in the Figure legends. In all experiments *p < 0.05, **p < 0.01, ***p < 0.001, ****p < 0.0001. Non-significant differences (n.s.) are generally not indicated.

Declarations

Funding Declaration

This work was funded in part by the MRC Confidence in Concept Award MC_PC_16056 (A.M.); VaxHub Global grant, Department of Health and Social Care using UK Aid funding, with support from EPSRC as part of the UK Vaccine Network (UKVN), a UK Aid programme to develop vaccines for diseases with

epidemic potential in low and middle-income countries (LMICs) (A.M); Chan Zuckerberg Initiative grant 2020-217289 (A.M., J.F.), UK Medical Research Council MR/Y004450/1 (J.F.); NIHR Biomedical Research Centre, Inflammation Across Tissues Theme (J.F.); the Kennedy Trust for Rheumatology Research KENN212202 (J.S.B.), Medical Research Council MR/W001217/1 (J.S.B.); and Kennedy Trust for Rheumatology Research Studentship (S.Q.), The Clarendon Fund in partnership with an Oxford-St Cross E.P. Abraham Scholarship and Nuffield Department of Clinical Medicine Studentship (L.S.), Michelson Prize 2022 (R.G.). S.R. was funded in part by the Deutsche Forschungsgemeinschaft (DFG, German Research Foundation, 495054088).

Acknowledgments

We thank Elena Stylianou for sharing the expertise on growing BCG and intradermal injections, and Mariya Mykhaylyk for lab-keeping assistance. H2-Kd *P. berghei* CSP 245-253 SYIPSAEKI tetramer was kindly provided by the NIH Tetramer Core Facility (contract number 75N93020D00005). Illustrations were created with BioRender.com.

Author Contribution (CRediT)

Conceptualization: JRF, AM

Methodology: SR, SQ, LS, JSB, AM

Validation: SR, JRF, AM

Formal analysis: SR, RG, JRF

Investigation: SR, MU, SQ, LS, RG, AT, JRF, AM

Resources: JSB, AM

Data Curation: SR, JRF, AM

Writing - Original Draft: SR

Writing - Review & Editing: SR, MU, SQ, LS, RG, JSB, JRF, AM

Visualization: SR

Supervision: AM

Project administration: JSB, JRF, AM

Funding acquisition: SR, JSB, AM

Declaration of Interest

The authors declare no competing interests.

References

1. Jurczak, M. & Druszczynska, M. Beyond Tuberculosis: The Surprising Immunological Benefits of the Bacillus Calmette-Guerin (BCG) Vaccine in Infectious, Auto-Immune, and Inflammatory Diseases. *Pathogens* 14, doi:10.3390/pathogens14020196 (2025).
2. Ochando, J., Mulder, W. J. M., Madsen, J. C., Netea, M. G. & Duivenvoorden, R. Trained immunity - basic concepts and contributions to immunopathology. *Nat Rev Nephrol* 19, 23–37, doi:10.1038/s41581-022-00633-5 (2023).
3. de Araujo, A., Mambelli, F., Sanches, R. O., Marinho, F. V. & Oliveira, S. C. Current Understanding of Bacillus Calmette-Guerin-Mediated Trained Immunity and Its Perspectives for Controlling Intracellular Infections. *Pathogens* 12, doi:10.3390/pathogens12121386 (2023).
4. Clark, I. A., Allison, A. C. & Cox, F. E. Protection of mice against Babesia and Plasmodium with BCG. *Nature* 259, 309–311, doi:10.1038/259309a0 (1976).
5. Matsumoto, S. *et al.* Mycobacterium bovis bacillus calmette-guerin induces protective immunity against infection by Plasmodium yoelii at blood-stage depending on shifting immunity toward Th1 type and inducing protective IgG2a after the parasite infection. *Vaccine* 19, 779–787, doi:10.1016/s0264-410x(00)00257-7 (2000).
6. Murphy, J. R. Host defenses in murine malaria: nonspecific resistance to Plasmodium berghei generated in response to Mycobacterium bovis infection or Corynebacterium parvum stimulation. *Infect Immun* 33, 199–211, doi:10.1128/iai.33.1.199-211.1981 (1981).
7. Parra, M. *et al.* Molecular analysis of non-specific protection against murine malaria induced by BCG vaccination. *PLoS One* 8, e66115, doi:10.1371/journal.pone.0066115 (2013).
8. Witschkowski, J. *et al.* BCG Provides Short-Term Protection from Experimental Cerebral Malaria in Mice. *Vaccines (Basel)* 8, doi:10.3390/vaccines8040745 (2020).
9. Berendsen, M. L. *et al.* BCG vaccination is associated with reduced malaria prevalence in children under the age of 5 years in sub-Saharan Africa. *BMJ Glob Health* 4, e001862, doi:10.1136/bmjgh-2019-001862 (2019).
10. Jensen, K. J. *et al.* Seasonal variation in the non-specific effects of BCG vaccination on neonatal mortality: three randomised controlled trials in Guinea-Bissau. *BMJ Glob Health* 5, e001873, doi:10.1136/bmjgh-2019-001873 (2020).
11. Hutchings, C. L., Birkett, A. J., Moore, A. C. & Hill, A. V. Combination of protein and viral vaccines induces potent cellular and humoral immune responses and enhanced protection from murine malaria challenge. *Infect Immun* 75, 5819–5826, doi:10.1128/IAI.00828-07 (2007).

12. Milicic, A. *et al.* Adjuvanting a viral vectored vaccine against pre-erythrocytic malaria. *Sci Rep* 7, 7284, doi:10.1038/s41598-017-07246-0 (2017).
13. Plebanski, M. *et al.* Protection from Plasmodium berghei infection by priming and boosting T cells to a single class I-restricted epitope with recombinant carriers suitable for human use. *Eur J Immunol* 28, 4345–4355, doi:10.1002/(SICI)1521-4141(199812)28:12%3C4345::AID-IMMU4345%3E3.0.CO;2-P (1998).
14. Baydemir, I., Dulfer, E. A., Netea, M. G. & Dominguez-Andres, J. Trained immunity-inducing vaccines: Harnessing innate memory for vaccine design and delivery. *Clin Immunol* 261, 109930, doi:10.1016/j.clim.2024.109930 (2024).
15. Fernandez-Ruiz, D. *et al.* Liver-Resident Memory CD8(+) T Cells Form a Front-Line Defense against Malaria Liver-Stage Infection. *Immunity* 45, 889–902, doi:10.1016/j.immuni.2016.08.011 (2016).
16. Sato, T. *et al.* Role for CXCR6 in recruitment of activated CD8 + lymphocytes to inflamed liver. *J Immunol* 174, 277–283, doi:10.4049/jimmunol.174.1.277 (2005).
17. Torracinta, L., Gogichadze, N. & Tanner, R. Immune mechanisms mediating the heterologous effects of BCG vaccination: a systematic review. *Front Immunol* 16, 1567111, doi:10.3389/fimmu.2025.1567111 (2025).
18. Atasheva, S. & Shayakhmetov, D. M. Cytokine Responses to Adenovirus and Adenovirus Vectors. *Viruses* 14, doi:10.3390/v14050888 (2022).
19. Chen, J. *et al.* BCG-induced trained immunity: history, mechanisms and potential applications. *J Transl Med* 21, 106, doi:10.1186/s12967-023-03944-8 (2023).
20. Reinke, S., Thakur, A., Gartlan, C., Bezbradica, J. S. & Milicic, A. Inflammasome-Mediated Immunogenicity of Clinical and Experimental Vaccine Adjuvants. *Vaccines (Basel)* 8, doi:10.3390/vaccines8030554 (2020).
21. de Araujo, A., de Queiroz, N., Marinho, F. V. & Oliveira, S. C. Bacillus Calmette-Guerin-Trained Macrophages Elicit a Protective Inflammatory Response against the Pathogenic Bacteria Brucella abortus. *J Immunol* 211, 791–803, doi:10.4049/jimmunol.2200642 (2023).
22. Teigler, J. E., Iampietro, M. J. & Barouch, D. H. Vaccination with adenovirus serotypes 35, 26, and 48 elicits higher levels of innate cytokine responses than adenovirus serotype 5 in rhesus monkeys. *J Virol* 86, 9590–9598, doi:10.1128/JVI.00740-12 (2012).
23. Huante, M. B. *et al.* Differential inflammasome activation signatures following intracellular infection of human macrophages with Mycobacterium bovis BCG or Trypanosoma cruzi. *Tuberculosis (Edinb)* 101S, S35-S44, doi:10.1016/j.tube.2016.09.026 (2016).
24. Hilligan, K. L. *et al.* Bacterial-induced or passively administered interferon gamma conditions the lung for early control of SARS-CoV-2. *Nat Commun* 14, 8229, doi:10.1038/s41467-023-43447-0 (2023).
25. Lee, A. *et al.* BCG vaccination stimulates integrated organ immunity by feedback of the adaptive immune response to imprint prolonged innate antiviral resistance. *Nat Immunol* 25, 41–53, doi:10.1038/s41590-023-01700-0 (2024).

26. Rakshit, S. *et al.* Evidence for the heterologous benefits of prior BCG vaccination on COVISHIELD vaccine-induced immune responses in SARS-CoV-2 seronegative young Indian adults. *Front Immunol* 13, 985938, doi:10.3389/fimmu.2022.985938 (2022).
27. Ramos-Martinez, E. *et al.* Effect of BCG Revaccination on Occupationally Exposed Medical Personnel Vaccinated against SARS-CoV-2. *Cells* 10, doi:10.3390/cells10113179 (2021).
28. Collins, K. A., Snaith, R., Cottingham, M. G., Gilbert, S. C. & Hill, A. V. S. Enhancing protective immunity to malaria with a highly immunogenic virus-like particle vaccine. *Sci Rep* 7, 46621, doi:10.1038/srep46621 (2017).
29. Reinke, S. *et al.* Emulsion and liposome-based adjuvanted R21 vaccine formulations mediate protection against malaria through distinct immune mechanisms. *Cell Rep Med* 4, 101245, doi:10.1016/j.xcrm.2023.101245 (2023).

Figures

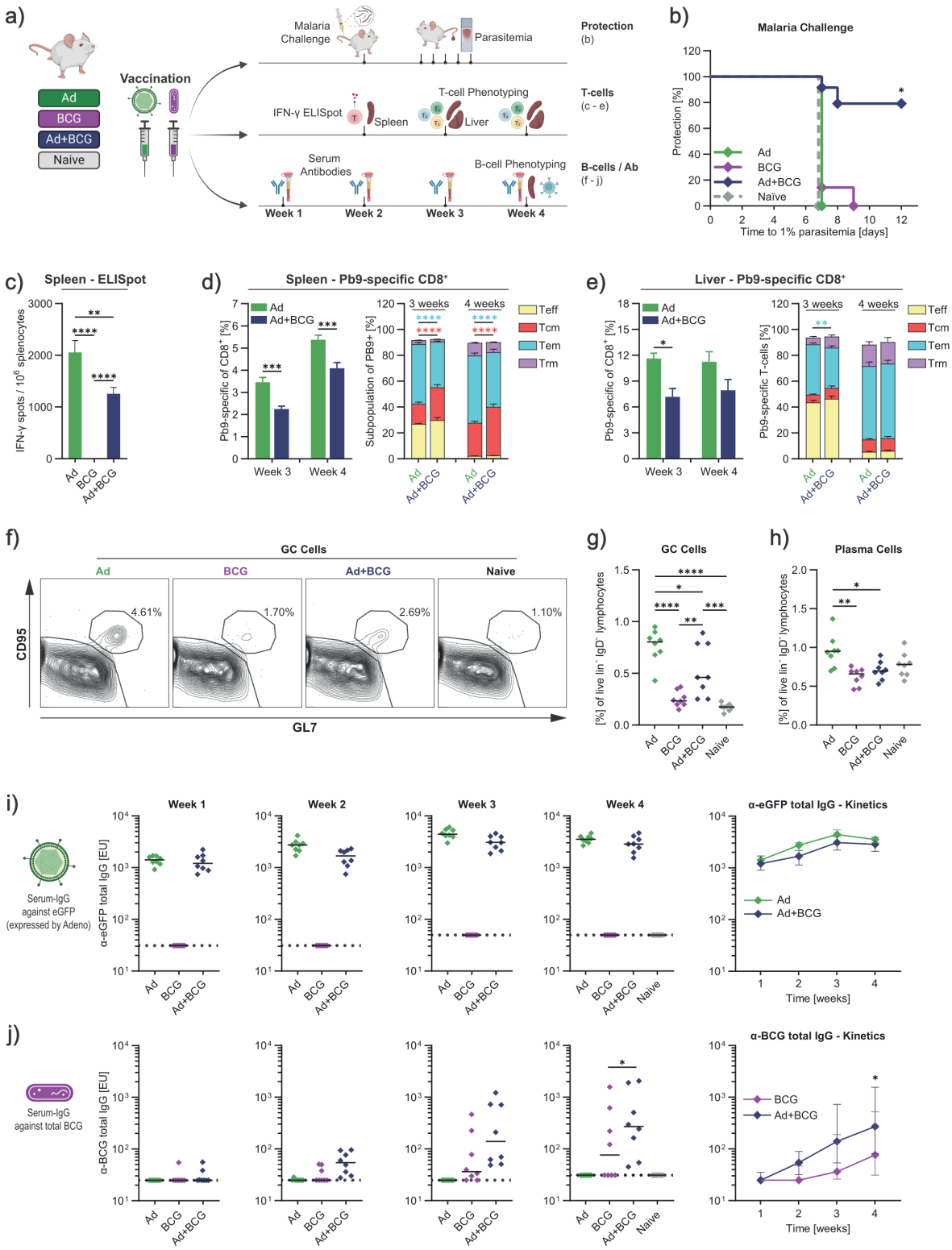


Figure 1

Ad+BCG co-administration enables protection against malaria in mice

(a) Summary of experimental design, indicating corresponding figure panels. Vaccine dose per mouse: $0.5x10^5$ CFU for BCG (i.d. or i.m.) and $5x10^7$ i.u. for AdHu5-TIPeGFP (i.m.).

(b) Survival post-malaria challenge: BALB/c mice were vaccinated and challenged as in (a). Parasitaemia was assessed by daily blood smears, with 1% parasitaemia taken as irreversible malaria infection. Ad+BCG vs. Ad or BCG alone: $p < 0.01$, pairwise fisher test with Bonferroni correction ($n \geq 7$).

(c) IFN-γ producing $CD8^+$ T cells in the spleen two weeks post-vaccination, restimulated with the Pb9 peptide for 20 h ex vivo. Data show the mean + SEM (n = 8); one-way ANOVA with Bonferroni's correction for multiple comparisons; **p < 0.01; ****p < 0.0001.

(d and e) T cell phenotyping in spleen and liver after vaccination and harvest as in (a). Left-hand panels show percentage of antigen (Ag) specific $CD8^+$ T cells 3 or 4 weeks after vaccination. Right-hand panels show the distribution of T cell subpopulations within the $Pb9^+$, $CD8^+$ compartment. Gating strategy as in figure S1d. Mean + SEM (n = 6); 2-way ANOVA with Bonferroni's correction for multiple comparisons; *p < 0.05; **p < 0.01; ***p < 0.001; ****p < 0.0001.

(f – h) Total B cell phenotyping of splenocytes after vaccination and harvest as in (a). **(f)** Representative FACS plots of $CD95^+$ $GL7^+$ germinal centre B cell populations, showing percentages of live IgD^-, lin^-, $CD138^-$, $B220^+$ lymphocytes. **(g)** Quantification of data presented in (f). Percentages of live IgD^-, lin^- lymphocytes. Each symbol represents an individual mouse (n = 8). **(h)** Quantification of plasma B cells after vaccination (n = 8). **(f-h)** Gating strategy as in figure S2d. Median + replicates; one-way ANOVA with Bonferroni's correction for multiple comparisons; *p < 0.05; **p < 0.01; ***p < 0.001; ****p < 0.0001.

(i) Serum anti-GFP IgG titres were measured by ELISA at the indicated time-points post immunisation; GFP is encoded by the Ad construct and used as a surrogate vaccine antigen. Each symbol represents an individual mouse (n = 8). Dashed line indicates the limit of detection. The panel on the right shows the anti-GFP antibody (Ab) titres over 4 weeks following vaccination.

(j) Serum anti-BCG IgG titres were measured by ELISA at the indicated time-points post immunisation. Each symbol represents an individual mouse (n = 8). Dashed line indicates the limit of detection. The panel on the right shows the anti-BCG Ab titres over 4 weeks post-vaccination. Testing for seroconversion at week 4 using Barnard's Unconditional Test; *p < 0.05.

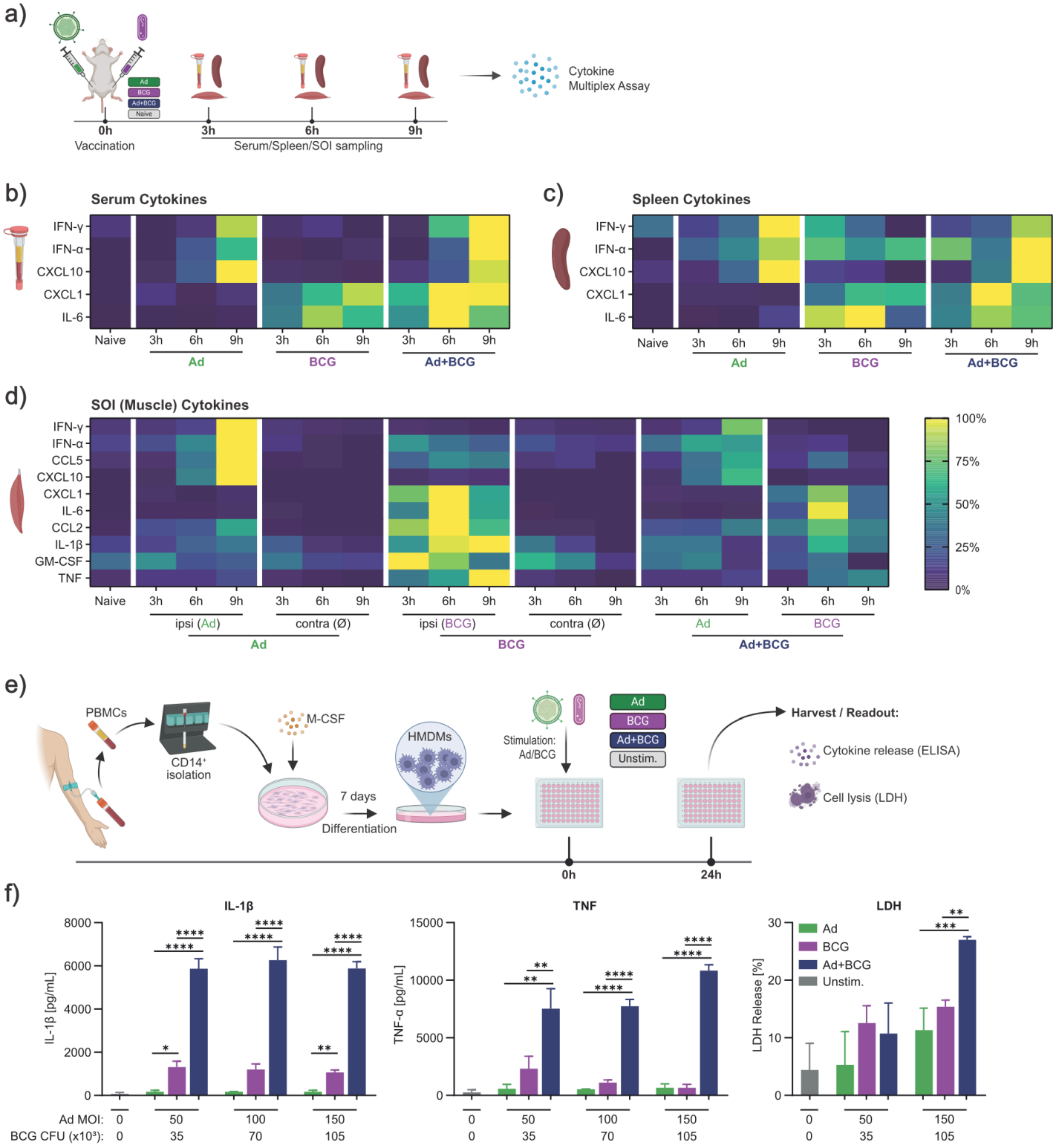


Figure 2

BCG broadens the systemic innate cytokine milieu

(a) Summary of the experimental design for data in (b-d). Vaccine dose per mouse: $0.5x10^5$ CFU for BCG and $5x10^7$ i.u. for AdHu5-TIPeGFP. In the Ad+BCG group, Ad was injected into the right leg and BCG into the left leg.

(b - d) Indicated cytokines were measured using LEGENDplex^{TM} MU Anti-Virus Response Panel. Heatmaps show relative cytokine levels detected in b) the serum, c) the spleen, and d) the ipsi- and contralateral muscle as the site of immunisation (SOI) for each vaccine (n = 6). Ad alone and BCG alone: contralateral leg received no vaccine, Ad+BCG: each leg received one of the vaccines. Individual cytokine kinetics are shown in figure S3.

(e) Summary of the experimental design for data in f).

(f) HMDMs were stimulated with Ad and/or BCG for 24 h at the indicated MOI/CFU. IL-1β and TNF secretion in supernatants was measured by ELISA. LDH release as a measure of lytic cell death was quantified using a colorimetric assay and is depicted as a percentage of the lysed positive control. Representative data from two independent experiments, showing stimulation triplicates. One-way ANOVA with Bonferroni's multiple comparison; *p < 0.05; **p < 0.01; ***p < 0.001; ****p < 0.0001.

Supplementary Files

This is a list of supplementary files associated with this preprint. Click to download.

- MilicicBCGAdSupplementaryMaterial.docx